Inter- and intra-subject variability of neuromagnetic resting state networks

Wens, Vincent; Bourguignon, Mathieu; Goldman, Serge; Marty, Brice; Op De Beeck, Marc; Clumeck, Catherine; Mary, Alison; Peigneux, Philippe; Van Bogaert, Patrick; Brookes, Matthew J.; De Tiège, Xavier

Published in:
Brain Topography

DOI:
10.1007/s10548-014-0364-8

Licence:
Other

Inter- and Intra-Subject Variability of Neuromagnetic Resting State Networks

Vincent Wens · Mathieu Bourguignon · Serge Goldman · Brice Marty · Marc Op de beeck · Catherine Clumeck · Alison Mary · Philippe Peigneux · Patrick Van Bogaert · Matthew J. Brookes · Xavier De Tiège

Received: 18 December 2013 / Accepted: 24 March 2014

Abstract Functional connectivity studies conducted at the group level using magnetoencephalography (MEG) suggest that resting state networks (RSNs) emerge from the large-scale envelope correlation structure within spontaneous oscillatory brain activity. However, little is known about the consistency of MEG RSNs at the individual level. This paper investigates the inter- and intra-subject variability of three MEG RSNs (sensorimotor, auditory and visual) using seed-based source space envelope correlation analysis applied to 5 minutes of resting state MEG data acquired from a 306-channel whole-scalp neuromagnetometer (Elekta Oy, Helsinki, Finland) and source projected with minimum norm estimation. The main finding is that these three MEG RSNs exhibit substantial variability at the single-subject level across and within individuals, which depends on the RSN type, but can be reduced after averaging over subjects or sessions. Over- and under-estimations of true RSNs variability are respectively obtained using template seeds, which are potentially mislocated due to inter-subject variations, and a seed optimization method minimizing variability. In particular, bounds on the minimal number of subjects or sessions required to obtain highly consistent between- or within-subject averages of MEG RSNs are derived. Furthermore, RSN topography positively correlates with their mean connectivity at the inter-subject level. These results indicate that MEG RSNs associated with primary cortices can be robustly extracted from seed-based envelope correlation and adequate averaging. MEG thus appears to be a valid technique to compare RSNs across subjects or conditions, at least when using the current methods.

Keywords Resting state networks · Functional connectivity · Brain oscillations · MEG · Variability

V. Wens · M. Bourguignon · S. Goldman · B. Marty · M. Op de Beeck · C. Clumeck · P. Van Bogaert · X. De Tiège
Laboratoire de Cartographie fonctionnelle du Cerveau, UNI–ULB Neurosciences Institute, Université libre de Bruxelles (ULB), Brussels, Belgium
E-mail: vwens@ulb.ac.be

M. Bourguignon
Brain Research Unit, O.V. Lounasmaa Laboratory, Aalto NeuroImaging, School of Science, Aalto University, FI-00076 AALTO, Espoo, Finland

A. Mary · P. Peigneux
UR2NF–Neuropsychology and Functional Neuroimaging Research Unit at CRCN–Centre de Recherches Cognition et Neurosciences, and UNI–ULB Neurosciences Institute, Université libre de Bruxelles (ULB), Brussels, Belgium

M. J. Brookes
Sir Peter Mansfield Magnetic Resonance Centre, School of Physics and Astronomy, University of Nottingham, University Park, Nottingham, United Kingdom

1 Introduction

The recent discovery of resting state networks (RSNs) undoubtedly represents a cornerstone in neuroscience, demonstrating that brain activity at rest does not merely amounts to background noise but may be functionally relevant (for reviews, see Deco and Corbetta (2011); Deco et al. (2011); Raichle (2010)). RSNs are large-scale distributed spatiotemporal structures that emerge in the spontaneous brain activity from the dynamic interaction between remote neural populations (for reviews, see Deco and Corbetta (2011); Deco et al. (2011)). Neuroimaging studies have disclosed the existence of RSN topographies that correspond to the sensorimotor, auditory or visual networks as well as networks involved in high-level associative processes such as the fronto-parietal, the executive or the default mode networks. Those RSNs are understood as background functional communication pathways that are related to the underlying structural connectivity, but deviate from it through dynamic fluctuations of resting state functional connectivity (rsFC) (for reviews, see

Deco et al. (2011); Hutchison et al. (2013)). These rsFC fluctuations seem to play a critical role for the retention of prior information, the processing of future stimuli and task-performance (for a review, see Deco and Corbetta (2011)). In addition, the observation of abnormal rsFC in various neurological or psychiatric disorders further supports the potential functional relevance of RSNs (for a review, see Fox and Greicius (2010)).

The main method for studying RSNs has been to apply rsFC metrics in the slow fluctuations (< 0.1 Hz) of spontaneous blood oxygen-level dependent (BOLD) signals as measured via functional magnetic resonance imaging (fMRI) (Biswal et al. 1995; Fox and Raichle 2007). Nevertheless, the hemodynamic basis of BOLD signal imposes two fundamental limitations. First, the effective low-pass filtering due to the hemodynamic response precludes investigations of fine temporal and spectral properties of RSNs. Second, the poorly understood nature of neurovascular coupling obscures the electrophysiological basis of the BOLD signal (Liu 2013). This latter caveat may be particularly confounding when studying rsFC modulations associated with changes in brain states or diseases, which may have a direct effect on the neurovascular coupling rather than neural activity per se (for reviews, see D'Esposito et al. (2003); Lindauer et al. (2010)). Fortunately, these two significant limitations can be overcome by using magnetoencephalography (MEG), an electrophysiological neuroimaging modality that measures magnetic fields induced by neuronal current flow. MEG offers excellent temporal resolution (1 ms) and, when combined with appropriate inverse modeling and structural MRI, also allows reconstruction of neural current sources with a reasonable spatial resolution (~ 5 mm) (Del Gratta et al. 2001; Hämäläinen et al. 1993). These properties of MEG as a neuroimaging modality, as well as its straightforward nature, make the derived signals rich in information, potentially yielding novel information on the electrophysiological basis of rsFC (for reviews, see Scholvinck et al. (2013); Hall et al. (2013a)).

RSNs that are spatially similar to those observed in fMRI have been evidenced with MEG by suitably adapting rsFC measurement to source localized MEG recordings. Independent component analysis (ICA) (Brookes et al. 2011; Brookes et al. 2012b; Hall et al. 2013b; Luckhoo et al. 2012b; Scholvinck et al. 2013) and seed-based correlation analysis (Brookes et al. 2012b; de Pasquale et al. 2010; Hipp et al. 2012), both applied to source space projected MEG data, have shown that the spatial signature of RSNs can emerge from temporal co-variation patterns in slow fluctuations (< 1 Hz) of band-limited amplitude (or power) envelopes estimated from ongoing electrical activity. This is somewhat distinct from the works on MEG rsFC that focus on phase synchronization (for a review, see Stam (2005)), although it is noteworthy that recent work (Marzetti et al. 2013) may offer a means to unify the two approaches. These findings begin to unveil an electrophysiological basis for RSNs and shed light on how neural oscillations may play an important role. Furthermore, the excellent temporal resolution and direct nature of MEG recordings allow investigation into the spectral content of RSNs (Brookes et al. 2011; Hipp et al. 2012) as well as their temporal non-stationarity (de Pasquale et al. 2010; de Pasquale et al. 2012), and to characterize task-related changes in their oscillatory activity (Brookes et al. 2012a; Luckhoo et al. 2012b). Band-limited MEG envelope rsFC also demonstrated its use for the investigation of neuropathological conditions (Hawellek et al. 2013).

To date, MEG RSN studies have primarily focused on group level analyses, and the important step of assessing test/re-test reliability and inter-individual variability in MEG RSNs is still missing. Uncovering MEG RSNs consistency across and within individuals may lead to a better knowledge of the neural mechanisms at the basis of RSNs emergence, as well as their functional relevance. Ultimately, it would also better determine the usefulness of MEG, within the armamentarium of functional neuroimaging techniques, to investigate RSNs for research or clinical purposes.

This paper therefore investigates the inter- and intra-subject variability of MEG RSNs in a large group of healthy adult subjects, focusing specifically on three RSNs associated with primary cortices (sensorimotor, auditory and visual) derived from the seed-based source envelope correlation analysis previously described (Brookes et al. 2012b; Hipp et al. 2012). First, the influence of inter- and intra-subject variability on single-subject and group level RSN maps is characterized. Second, this work examines the relation between RSN topography and various parameters such as their connectivity and band-limited power levels, the moment of resting state data acquisition, as well as the effect of raw MEG data quality or the embedding of resting state sessions amongst task-related conditions. Finally, since RSNs variability obtained using template seeds common to all subjects may be over-estimated because of, e.g., seed mislocation, under-estimation was also obtained using an individual-level seed optimization method. Comparison of these two approaches offers better insight into true MEG RSNs variability.

2 Materials and Methods

2.1 Subjects

Fifty-eight healthy adult subjects (31 females and 27 males, mean age: 24.5 years, age range: 18 to 38 years) performed a single resting state MEG session of 5 minutes (henceforth referred to as the single session data). Data were gathered from 4 studies (number of subjects per study: 9, 10, 15, 24), each of which being conducted by a different experimenter

and containing one resting state session amongst other task- or stimulus-driven sessions (for details, see supplementary material S6).

Four right-handed healthy adult subjects (1 female and 3 males, mean age 31 years, age range: 27 to 37 years) also performed 20 resting state MEG sessions of 5 minutes in one day (henceforth referred to as the multiple sessions data). Two consecutive sessions were separated by approximately 15 minutes during which subjects performed various daily activities outside the MEG.

No subject had a history of neurologic or psychiatric disease and all were right-handed as assessed by the Edinburgh Handedness Inventory (Oldfield 1971). They participated after written informed consent. All studies were approved by the ULB-Hpital Erasme Ethics Committee.

2.2 Data acquisition and preprocessing

MEG data were recorded in a magnetically shielded room (Maxshieldł, Elekta Oy, Helsinki, Finland) using a 306-channel whole-scalp-covering neuromagnetometer (Vectorview, Elekta Oy, Helsinki, Finland) installed at the ULB-Hôpital Erasme (Carrette et al. 2011; De Tiège et al. 2008). During 5 minutes, subjects were asked to sit still while gazing at a fixation cross on a screen (15 subjects, single session) or a point on the opposite wall of the magnetically shielded room (43 subjects, single session; 4 subjects, multiple sessions). MEG data were sampled at 1 kHz and bandpass-filtered at 0.1–330 Hz. Four head-tracking coils monitored subjects' head position inside the MEG helmet. The locations of the coils and at least 150 head-surface (on scalp, nose and face) points with respect to anatomical fiducials were recorded with an electromagnetic tracker (Fastrak, Polhemus, Colchester, VT, USA). Subject's high-resolution 3D-T1 weighted MRI were also acquired using a 1.5 T MRI scanner (Intera, Philips, The Netherlands).

The raw MEG data were preprocessed off-line using the signal space separation method (Taulu et al. 2005) to subtract external interferences and correct for head movements. Cardiac, eye-movement and electronic artifacts were removed by ICA (Vigario et al. 2000) and visual inspection applied to sensor time series filtered between 0.5 and 45 Hz (number of removed components per subject: mean 3.6, range 2–8). Cleaned data were then filtered into the θ (4–8 Hz), α (8–12 Hz) and β (12–30 Hz) bands.

2.3 Source reconstruction

Individual anatomical MRIs were segmented using the Freesurfer software (Martinos Center for Biomedical Imaging, Massachusetts, USA). MEG and segmented MRI coordinate systems were co-registered using the three anatomical fiducial points for initial estimation and the head-surface points to manually refine the surface co-registration. Individual MEG forward models were then computed using the Boundary Element Method implemented in the MNE software suite (Martinos Center for Biomedical Imaging, Massachusetts, USA). To enable between-subject and group comparisons, forward models were based on a source grid obtained from a common regular 5-mm grid defined on the Montreal Neurological Institute (MNI) template brain by applying a non-linear spatial deformation algorithm implemented in Statistical Parametric Mapping (SPM8, Wellcome Department of Cognitive Neurology, London, UK).

Inverse modeling was performed with a band-specific weighted Minimum Norm Estimate (wMNE) (Dale and Sereno 1993) using gradiometer signals only to increase signal-to-noise ratio and minimize the potential difficulties associated with signal space separation (Luckhoo et al. 2012a). For each frequency band, sensor-space noise covariance was estimated from 5 minutes of artifact-free data recorded from an empty room and filtered into the relevant frequency bands. The wMNE regularization parameter was fixed using an estimate of the signal to noise ratio as prescribed in Hämäläinen et al. (2010). The resulting inverse operator was applied to the cleaned MEG data filtered in the associated band. The dimension of each dipole moment was reduced from 3 to 1 by projection onto the direction of maximum variance, which defined the power of the resulting source time series. Finally, the analytic signal was derived using the Hilbert transform.

2.4 Seed-based correlation analysis

The connectivity method used in this work was adapted from the seed-based correlation analysis described in Brookes et al. (2012b) and Hipp et al. (2012), but based upon source reconstruction using wMNE, which has been used in similar MEG functional connectivity work (de Pasquale et al. 2010; de Pasquale et al. 2012). First, linear signal leakage from the seed location, which gives rise to spurious connectivity, was corrected via orthogonalization of each source's analytic signal with respect to the seed's analytic signal (Hipp et al. 2012). Then, the envelope of the seed and of the leakage corrected sources was estimated by taking the modulus of their analytic signal, and slow fluctuations (< 1 Hz) were extracted by averaging over 1 s-long windows. Finally, the Pearson correlation coefficient was computed between the slow envelope fluctuations of the seed and of each corrected source, hence resulting in a seed-based connectivity map. Of notice, the reported connectivity levels were not corrected for the envelope correlation underestimation bias induced by orthogonalization. According to Hipp et al. (2012), true connectivity values are recovered upon multiplication by a

factor of $\sqrt{3}$. In any case, the absence of correction did not affect the analyses performed in this paper.

The seeds were placed in the left primary sensorimotor (SM1), auditory (A1) and visual (V1) cortices for the homonymous RSNs. Based upon a previous publication (Hipp et al. 2012), the template MNI coordinates defining the location of these seeds and the frequency bands employed to extract individual and group level RSNs were chosen as follows: SM1: $[-42,-26,54]$ mm, β band; A1: $[-54,-22,10]$ mm, β band; V1: $[-20,-86,18]$ mm, α band. To reduce inter-subject variations potentially associated with variability in structural or functional anatomy, individual RSNs were also extracted for each seed comprised in a region of interest centered on those coordinates (SM1 and V1: sphere with radius $R = 15$ mm; A1: ellipsoid with semi-principal axes lengths $R_x = 24$ mm, $R_y = R_z = 12$ mm; see supplementary material S1) and subsequently subjected to an optimization process described below.

2.5 Variability of individual MEG RSNs

2.5.1 Group level connectivity maps

Single-subject envelope connectivity maps were derived from the 58 single sessions, yielding 58 maps (one per subject) for each of the 3 considered MNI template seeds. Group level connectivity maps were obtained by averaging over the 58 maps. The resulting group level maps were taken as canonical representations of the 3 MEG RSNs investigated in this study, and will henceforth be referred to as the "canonical maps" or "canonical RSNs".

2.5.2 Consistency of individual RSN topography

The consistency of individual RSN topography was assessed using their spatial similarity with the corresponding canonical RSN. Spatial similarity is defined as the spatial Pearson correlation coefficient between the individual connectivity map and its associated canonical map, and characterizes the topographical quality of an individual RSN. To avoid the bias of a spatial similarity driven only by high levels of connectivity in a single hemisphere, an additional index focusing on inter-hemispheric rsFC was derived from the maps restricted to the hemisphere contralateral to the seed (right-hemisphere in this case). These two indices will henceforth be referred to as "whole-brain spatial similarity" (r_{whole}) for the former and as "right-hemisphere spatial similarity" (r_{right}) for the latter. The dependence of individual maps spatial similarities on the RSN (SM1, A1 and V1) was tested using a non-parametric Kruskal-Wallis one-way ANOVA with the RSN as a factor, and specific differences between RSNs were then investigated post-hoc using non-parametric one-sided t-tests based on null distributions generated via 10^5 permutations of the 58 subjects.

2.5.3 Dependence of RSN topography on mean connectivity and power levels

Spatial similarity indices yielded topographical information about individual RSNs topography that was a priori distinct from their mean connectivity level. Therefore, within-network connectivity was also computed, for each individual map, by averaging the envelope correlation coefficients over the 25% of sources with largest values in the associated canonical connectivity map, which allowed proper delimitation of the regions involved in each RSN. Similarly, within-network power levels in the θ, α and β bands were computed by averaging individual band-limited source power levels over the same masks. Since an absence of correlation with band-limited power levels does not preclude a relation with their ratios, which are known to be predictive of the subject's state of vigilance, the ratios between within-network power levels in the different frequency bands (α/θ, α/β and θ/β) were also calculated. The existence of a relation between spatial similarities and these connectivity/power indices was tested using Spearman rank correlation. In the case of within-network connectivity level, a sigmoid-based model $r = a\tanh(b\rho + c)$ of whole-brain spatial similarity r as a function of within-network connectivity level ρ, was also fitted to these data using a standard least-square criterion.

2.5.4 Consistency of group level RSN topography

The consistency of group level RSNs as a function of the number N of subjects used to estimate group averages was evaluated using a resampling approach. For each integer N from 2 to 30, 1000 distinct subpopulations of size N were generated by randomly picking N amongst the 58 subjects without replacements. Individual connectivity maps were then averaged over each subpopulation, yielding 1000 samples of size N group level maps. Their spatial similarities with the associated canonical map were then derived. The number of subjects required to obtain reliable RSNs topography across subpopulations was heuristically estimated as the smallest N such that the mean minus one standard deviation of whole-brain and right-hemisphere spatial similarities be simultaneously above 0.9. This high correlation threshold indeed ensured highly consistent size N group level maps across samples, and thus conservative estimation of N.

2.5.5 Seed optimization

Since the primary cortices structural and functional anatomy may differ at the individual level from the template seeds,

leading to potential over-estimation of RSNs variability, an optimization procedure based upon spatial similarity indices was implemented in order to minimize RSNs variability as much as possible. For each subject and RSN, connectivity maps were computed using orthogonalized slow envelope correlation, for each seed in the corresponding region of interest (see Section 2.4 and supplementary material S1). This resulted in a large number of connectivity maps per subject and RSN. Their spatial similarities with the canonical map were derived, and the map with the highest mean spatial similarity ($r_{\text{mean}} = (r_{\text{whole}} + r_{\text{right}})/2$) was selected as the optimized individual RSN. The above analyses (Sections 2.5.2–2.5.4) were then carried over using the resulting maps based on optimized seeds.

2.6 Intra-subject and inter-subject variability of MEG RSNs

2.6.1 Multiple sessions connectivity maps and within-subject averages

Intra-subject variability was assessed using the multiple sessions data obtained in 4 subjects. For each subject, connectivity maps were derived for each session from template seed-based envelope correlation analysis, yielding a total of 20 maps per subject for each RSN. Within-subject average connectivity maps, in which intra-subject (or inter-session) fluctuations are smoothed out, were then obtained by averaging over the 20 sessions.

2.6.2 Consistency of multiple sessions RSN topography (intra-subject variability)

The consistency of individual RSN topography across sessions was assessed using whole-brain and right-hemisphere spatial similarities of each multiple sessions connectivity-map with their associated canonical map. Furthermore, to enable a truly within-subject analysis and avoid reference to canonical maps, the whole-brain and right-hemisphere spatial correlations between each multiple sessions map and their associated within-subject average were also computed. The latter indices will henceforth be referred to as within-subject spatial similarities. The dependence of spatial similarities on the subject and on the RSN was tested using non-parametric Kruskal-Wallis one-way ANOVA tests.

2.6.3 Dependence of multiple sessions RSN topography on time

To test for the existence of temporal structure in the multiple sessions RSNs within each subject, a turning point test for whiteness (see, e.g., Brockwell and Davis (1987)) was applied, within each subject, to both whole-brain and right-hemisphere within-subject spatial similarities expressed as a function of time, to check if they significantly deviated from mere white processes. The idea of this test is to count the number of local extrema (turning points) in the time series and check if this number is significantly different from its expectation value for a white process. The null distribution of this statistic presents universal features; i.e., it only depends on the whiteness assumption and on the number n of time samples, has known mean and variance, and converges to a Gaussian in the large n limit. However, in our case n is rather small ($n = 20$), so the null distribution was non-parametrically generated using 10^5 random permutations of the n time samples. The result was also necessary to justify the applicability of the resampling analysis described next.

2.6.4 Consistency of within-subject average RSN topography

To investigate the consistency of within-subject average connectivity maps as a function of the number N of sessions used to average multiple sessions maps and dampen intra-subject fluctuations, a resampling analysis similar to that of Section 2.5.5 was performed within each of the 4 subjects. For each integer N from 2 to 18, 150 distinct subsets of N resting state sessions were picked randomly without replacement amongst the 20 available sessions, and connectivity maps were averaged over each of these subsets, yielding 150 samples of N-sessions maps. Their within-subject spatial similarities with the associated within-subject average maps (corresponding to $N = 20$) were then derived. The number of sessions required to obtain reliable individual average RSN topography across subsets was heuristically estimated as the smallest N such that the mean minus one standard deviation of whole-brain and right-hemisphere within-subject spatial similarities be simultaneously above 0.9. The independence assumption on the sample maps needed for this resampling analysis requires the absence of temporal structure in within-subject spatial similarities; this hypothesis was therefore first checked (see Section 2.6.3) before proceeding.

2.6.5 Seed optimization

A seed optimization procedure similar to that of Section 2.5.5 was also applied to each subject and session of the multiple sessions data, in order to bias connectivity maps towards the canonical RSNs as much as possible.

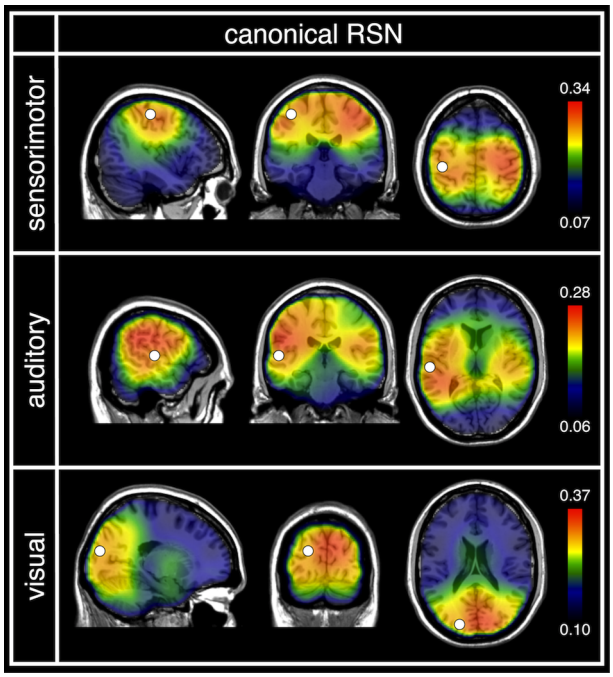

Fig. 1 Canonical connectivity maps superimposed on the MNI brain. The template seeds are indicated with white dots. The lower and upper thresholds were respectively fixed at the minimum and maximum of connectivity. The envelope correlation values indicated are uncorrected for the orthogonalization bias (Hipp et al. 2012)

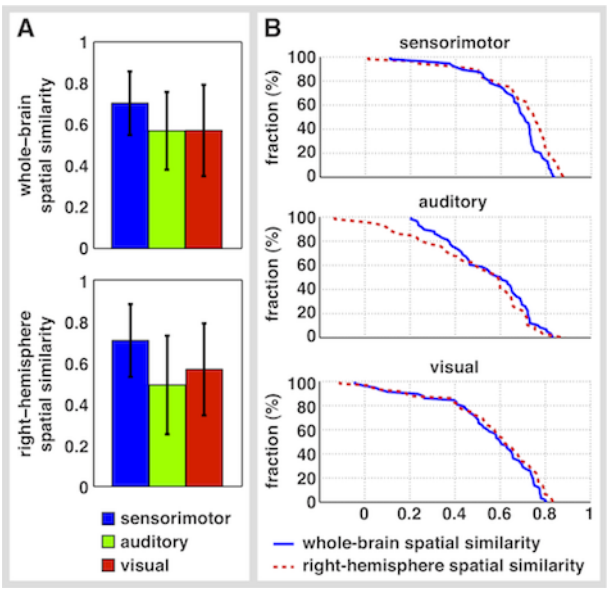

Fig. 2 Mean ± standard deviation (computed across 58 subjects) of whole-brain and right-hemisphere spatial similarities between single session individual connectivity maps and canonical maps (**A**), and fraction of subjects presenting spatial similarities above given values r (**B**). Mathematically, the latter curves are determined from the cumulative distribution functions $F(r)$ of each spatial similarity index via the formula $1 - F(r)$, and thus give a full description of their distribution

3 Results

3.1 Variability of individual MEG RSNs

3.1.1 Canonical RSNs

Figure 1 illustrates, for each considered RSN, the canonical maps obtained from template seeds, which were used for the spatial similarity analyses and for seed optimization. Typical inter-hemispheric connectivity was observed within each network (left SM1 to right SM1, left A1 to right A1, left V1 to right V1).

3.1.2 Consistency of individual RSN topography

The consistency and variability of single session connectivity maps are summarized in Figure 2, which shows the distribution of whole brain and right-hemisphere spatial similarities for each RSN across the 58 subjects. Figure 2A presents their mean and standard deviation, whereas Figure 2B gives the fraction of subjects with spatial similarities above given values. Qualitatively, these distributions indicate that RSNs topography is fairly variable across subjects for all RSNs. For example, Figure 2B indicates that, amongst the subjects, only 58% of the SM1 maps, 14% of the A1 maps and 29% of the V1 maps presented both spatial similarities above 0.7. Two extreme examples of individual maps are presented for each RSN in the supplementary material (left part of Figure S2).

The ANOVA tests on spatial similarity indices revealed an effect of the RSN type ($p < 4 \times 10^{-5}$). Post-hoc analysis at significance level 0.05 showed that the SM1 RSN presented higher spatial similarities than the other RSNs, and that the V1 RSN had higher right-hemisphere spatial similarity than the A1 RSN, but with no difference between their whole-brain spatial similarities (see Figure 2A).

3.1.3 Dependence of RSN topography on mean connectivity levels

Inter-subject fluctuations in spatial similarities are related to those in within-network connectivity levels. Indeed, both whole-brain and right-hemisphere spatial similarities increased monotonically with within-network connectivity levels ($p < 10^{-6}$ for all RSNs, Spearman correlation test) in a sigmoid fashion, as illustrated and modeled in Figure 3.

3.1.4 Dependence of RSN topography on mean power levels

After Bonferroni correction for $n = 12$ comparisons (2 spatial similarities $\times$ 6 power levels and ratios), significant power correlates of whole-brain and right-hemisphere spatial similarities were found only with the α/θ and α/β power ratios in the V1 RSN (positive Spearman correlation, $p < 4 \times$

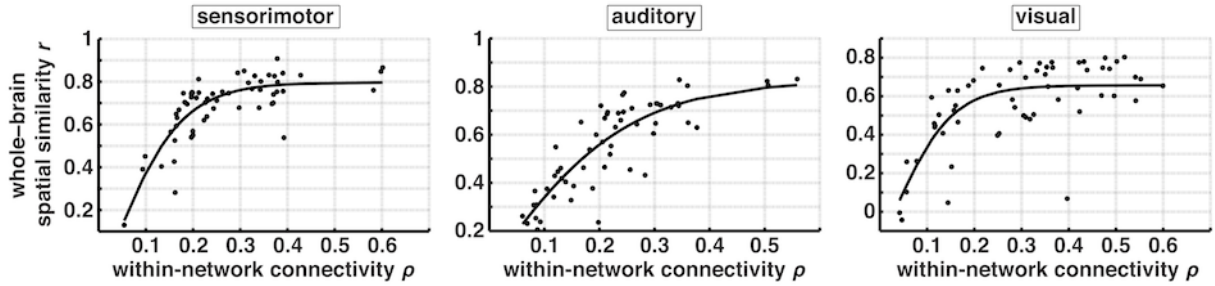

Fig. 3 Whole-brain spatial similarity r of individual (single session) connectivity maps with the associated canonical maps, as a function of their within-network connectivity level ρ. For each RSN, a model based on the sigmoid $r(\rho) = a\tanh(b\rho + c)$ was fitted (SM1: $a = 0.80$, $b = 6.91$, $c = 0.09$, $\sigma_\varepsilon = 0.09$; A1: $a = 0.83$, $b = 3.86$, $c = 0.05$, $\sigma_\varepsilon = 0.10$; V1: $a = 0.66$, $b = 8.19$, $c = -0.25$, $\sigma_\varepsilon = 0.15$; where σ_ε is the standard deviation of the model error $\varepsilon = r - r(\rho)$). When ρ is low enough, r increases approximately linearly with ρ, until the sigmoid saturates at the maximal value of r given by the model parameter a. The saturation domain $\rho_s \leq \rho \leq 1$, where $r \approx a$ becomes independent of ρ, can be approximated as the interval in which $r(\rho)$ is at least 99% of a (SM1: $\rho_s = 0.37$; A1: $\rho_s = 0.67$; V1: $\rho_s = 0.35$). Results for right-hemisphere spatial similarity are analogous

10^{-4}, uncorrected), showing that the larger these ratios are, the higher is the V1 RSN spatial similarity. Without correction, a tendency for significance was also observed between both spatial similarities and the α power in the V1 RSN and the β power and β/θ power ratio in the A1 RSN ($p < 0.06$, uncorrected). All other correlations had uncorrected p-values above 0.10. See also supplementary material S3 for further related tests.

3.1.5 Robustness of group level RSN topography

Figure 4 depicts the mean and standard deviation of spatial similarities plotted as a function of the population size N. This description of RSNs variability is actually redundant (see supplementary material S4), but allowed quantifying how group averaging dampens inter-subject fluctuations. The criterion given in Section 2.5.4 yielded the following minimum numbers of subjects necessary to obtain highly consistent size N group level maps: $N = 6$ for the SM1 RSN, $N = 12$ for the A1 RSN and $N = 10$ for the V1 RSN. See supplementary material (right part of Figure S2) to check the group maps with the lowest spatial similarities among the 1000 group maps obtained using the resampling analysis.

3.1.6 Relation between RSN topography and other parameters

See supplementary material for further statistical tests reporting no effect of raw MEG data quality (S5) or of embedding resting state session amongst task-related conditions (S6) on RSNs spatial similarities.

3.1.7 Effect of seed optimization

The effect of the seed optimization procedure on the consistency and variability of single session connectivity maps is illustrated in Figure 5, which compares the distribution of whole brain and right-hemisphere spatial similarities for each RSN across the 58 subjects, using optimized versus template seeds. Figure 2A presents their mean and standard deviation, whereas Figure 2B gives the fraction of subjects with spatial similarities above given values. Qualitatively, this indicates that optimized maps have higher spatial similarities and thus decreased variability. For example, Figure 2B indicates that the fraction of subjects with both spatial similarities above 0.7 increased to 84% for the SM1 RSN and 48% for the A1 and V1 RSNs. Likewise, the estimate of the minimum number of subjects necessary to obtain highly consistent size N group level maps decreased to $N = 4$ for the SM1 RSN and $N = 7$ for the A1 and V1 RSNs (see also supplementary material, Figure S7). The various tests described in the preceding sections disclosed qualitatively similar results and will not be further described here.

3.2 Intra-subject and inter-subject variability

3.2.1 Within-subject average RSNs

Figure 6 shows the within-subject average connectivity maps obtained by averaging over the 20 sessions within each subject that performed multiple resting state sessions. The SM1 maps exhibited the typical inter-hemispheric connectivity between left and right SM1 in all subjects, although with more diffuse and noisier connectivity patterns. In the A1 maps, the inter-hemispheric connectivity between left and right A1 was observed in subjects 2 and 3 but absent from the 2 others. Finally, in the V1 maps, the inter-hemispheric connectivity between left and right V1 was observed in all subjects but subject 2.

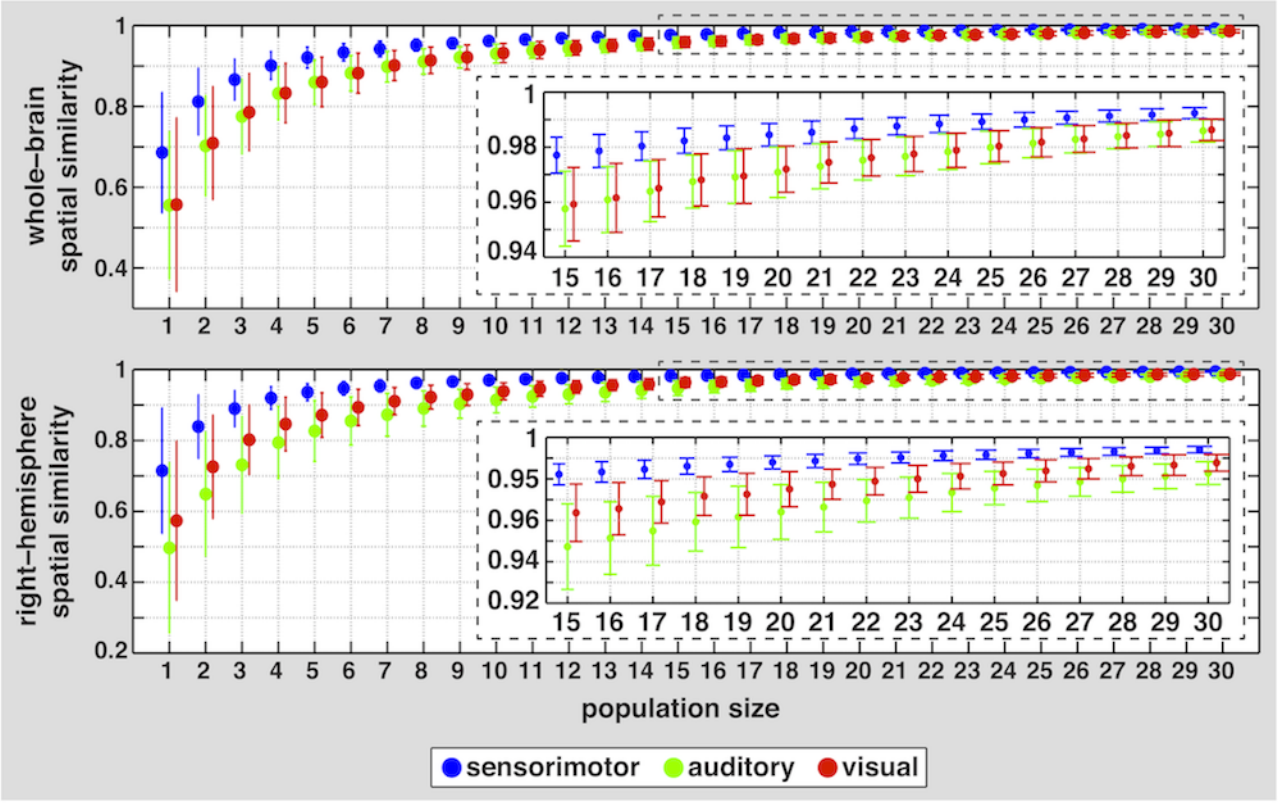

Fig. 4 Mean ± standard deviation of whole-brain (*top*) and right-hemisphere (*bottom*) spatial similarities between size N group connectivity maps ($1 \leq N \leq 30$) derived from optimized seeds and their associated canonical map, as a function of the population size N. The means and standard deviations were estimated using single sessions obtained in 58 subjects ($N = 1$) or 1000 randomly chosen subpopulations ($N \geq 2$). The insets zoom on values of $N \geq 15$

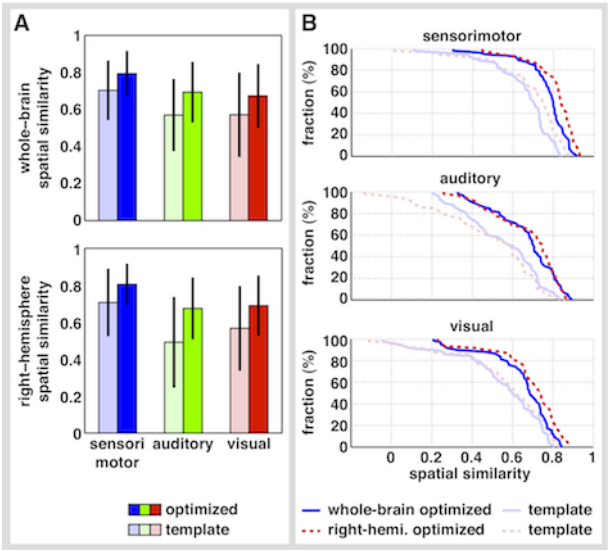

Fig. 5 Comparison of the distributions across subjects of whole-brain and right-hemisphere spatial similarities between single session individual connectivity maps and canonical maps, with and without seed optimization. The means and standard deviations were computed across 58 subjects (**A**). The fraction of subjects presenting spatial similarities above given values r were obtained from their cumulative distribution functions $F(r)$ via the formula $1 - F(r)$ (**B**)

3.2.2 Robustness of multiple sessions RSN topography (intra-subject variability)

The robustness and variability of multiple sessions connectivity maps are illustrated in Figure 7, which shows the distribution of whole-brain and right-hemisphere within-subject spatial similarities across the 20 sessions, for each RSN and each subject. Figure 7A presents the mean and standard deviation over sessions, whereas Figure 7B gives the mean and standard deviation over the 4 subjects of the fraction of sessions with within-subject spatial similarities above given values. Qualitatively, this indicates good consistency and low variability of RSNs across sessions, especially for the SM1 and A1 RSNs. For example, it follows from the distributions plotted in Figure 7B that, amongst the 20 sessions, 95% ± 4% of the SM1 maps, 78% ± 18% of the A1 maps and 49% ± 38% of the V1 maps (mean ± standard deviation, calculated over subjects) have both whole-brain and right-hemisphere within-subject spatial similarities above 0.7. Similar plots for spatial similarities with canonical RSNs (see supplementary material, Figure S8) suggest the existence of significant variations across subjects on top of variations across sessions, especially in the V1 RSN.

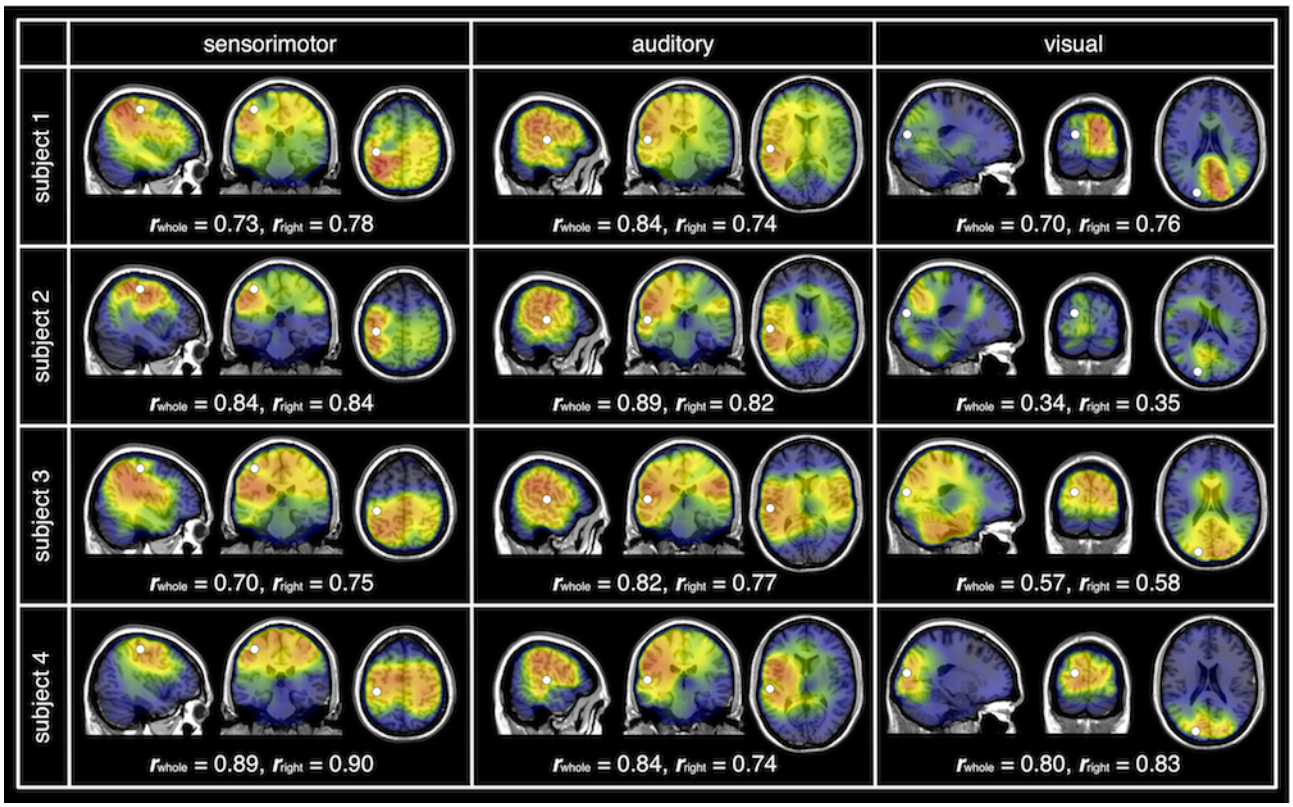

Fig. 6 Within-subject average connectivity maps derived from 20 sessions using seed optimization and superimposed on the MNI brain. The seeds are indicated with white dots. The lower and upper thresholds were respectively fixed at the minimum and maximum of connectivity. The values of the RSNs whole-brain (r_{whole}) and right-hemisphere (r_{right}) spatial similarities with the associated canonical RSN are also indicated

The ANOVA tests revealed a dependence on the subject for both spatial similarities in the SM1 and V1 RSNs ($p < 10^{-5}$, uncorrected), a tendency for right-hemisphere spatial similarity in the A1 RSN ($p = 0.04$, uncorrected), and none for whole-brain spatial similarity in the A1 RSN ($p = 0.19$, uncorrected). Spatial similarities also depended on the RSN ($p < 4 \times 10^{-4}$, uncorrected), but with post-hoc differences that varied from subject to subject without clear pattern.

3.2.3 Dependence of multiple sessions RSN topography on time

The turning point test for whiteness was not able to reject the null hypothesis (i.e., no temporal structure) either in whole-brain or right-hemisphere within-subject spatial similarity time series ($p > 0.08$, uncorrected). An exception arose in one subject, which had $p = 0.02$ (uncorrected) for whole-brain within-subject spatial similarity in the A1 RSN. However, in view of the multiple comparisons involved and of the fact that the associated right-hemisphere index presented a very large uncorrected p-value ($p = 0.60$), the hypothesis that RSNs are temporally independent (white) was not rejected.

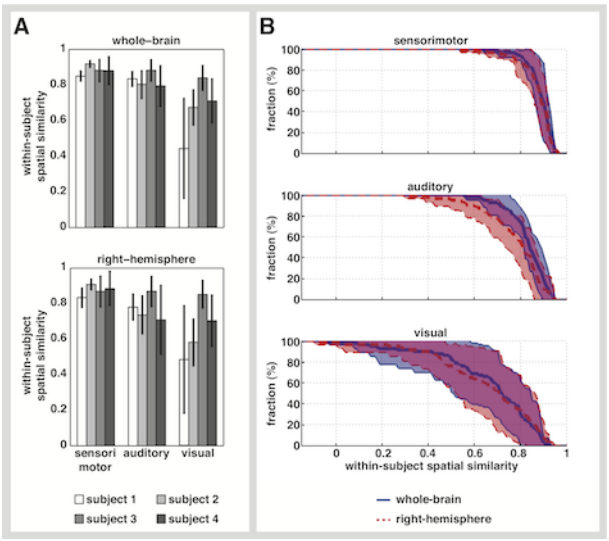

Fig. 7 Mean ± standard deviation (computed across 20 sessions, within each subject) of whole-brain and right-hemisphere within-subject spatial similarities between single session individual connectivity maps and their within-subject average (**A**), and mean ± standard deviation (computed across 4 subjects) of the fraction of sessions presenting spatial similarities above given values r (**B**). Mathematically, the latter curves are determined from the cumulative distribution functions $F(r)$ of each spatial similarity index via the formula $1 - F(r)$, and thus give a full description of their distribution across sessions, within each of the 4 subjects

3.2.4 Consistency of within-subject average RSN topography

Figure 8 plots, for each subject and each RSN, the mean and standard deviation of whole-brain and right-hemisphere within-subject spatial similarities of average maps as a function of the number N of sessions used to perform the average. It contains a redundancy similar to that previously described (see supplementary material, Figure S4) but allows to quantify how averaging over sessions dampens intra-subject fluctuations. The criterion given in Section 2.6.4 yielded the following minimal number of sessions necessary to obtain highly reliable within-subject average maps: $2 \leq N \leq 3$ for the SM1 RSN, $2 \leq N \leq 5$ for the A1 RSN and $3 \leq N \leq 11$ for the V1 RSN (range for the 4 subjects).

3.2.5 Relations between multiple sessions RSN topography and mean connectivity and power levels

See supplementary material S9 for further statistical tests reporting no clear patterns relating within-subject spatial similarities and mean connectivity or power at the intra-subject level.

3.2.6 Effect of seed optimization

The effect of the seed optimization procedure improved the robustness of single session and multiple sessions RSNs. For example, the minimal number of sessions required to obtain highly reliable within-subject average maps (as defined by the criterion in Section 2.6.4) decreased to $N = 2$ for the SM1 RSN, $2 \leq N \leq 3$ for the A1 RSN and $3 \leq N \leq 7$ for the V1 RSN (range for the 4 subjects) (see supplementary material, Figure S10).

4 Discussion

This study demonstrates that single-subject MEG RSNs derived from template seeds chosen in the SM1, A1 and V1 cortices exhibit substantial variability in their topography both across and within individuals. This variability depends on the RSN type, the SM1 RSN being the more robust. Apart from a clear correlation with mean RSN connectivity at the inter-subject level, neither the raw MEG data quality, the experimental condition, nor the moment of resting state acquisition is associated with the quality of MEG RSN topography. Furthermore, band-specific power levels or their ratios do not relate to RSN topography, except for the V1 RSN topography that is related to α/θ and α/β power ratios at the inter-subject level. Estimates for the number of subjects or sessions required to obtain highly consistent between- or within-subject averages of MEG RSNs are also given.

4.1 Variability of individual MEG RSNs

This study shows the existence of a substantial variability both in the topography and the connectivity level of individual RSNs when using template MNI seeds.

The topographical quality of single session connectivity maps was assessed here using spatial similarity indices. Whole-brain spatial similarity gives a concise global comparison with the canonical RSNs, whereas right-hemisphere spatial similarity focuses on inter-hemispheric rsFC patterns that are typical of networks associated with primary cortices. The distribution of these two indices across subjects was then used to quantify the variability that affects individual maps topographies. The SM1 RSN was found to be the most robust, whereas the A1 and V1 RSNs were more variable across subjects.

Importantly, the validity of this analysis based on spatial similarity indices requires that canonical RSNs, defined here via group averaging, accurately represent the underlying RSNs. This assumption was taken as valid, since the canonical RSNs obtained in this study were very similar to the MEG RSNs previously described (Brookes et al. 2011; Brookes et al. 2012b; Hipp et al. 2012); e.g., compare Figure 1 with Figures 2b, 2c, 2d in Hipp et al. (2012). Of notice, there were two major differences in the methods used in this paper compared to these previous works. First, resting state data were obtained using 204 planar gradiometers from an Elekta Neuromag MEG system instead of 275 axial gradiometers from CTF MEG systems. That RSNs can be reproduced using an Elekta Neuromag MEG was first shown by Luckhoo et al. (2012a) using ICA and both magnetometers and gradiometers. This paper presents a similar conclusion but using seed-based connectivity maps. Second, inverse modeling was based on wMNE, as in de Pasquale et al. (2010), rather than Beamforming. Despite the differences in their underlying hypotheses, group map topographies qualitatively converged. A more systematic comparison of these two methodologies was recently performed by O'Neill et al. (2013). These observations therefore argue for the robustness of group level MEG RSNs against data acquisition and source reconstruction methods. However, it should be stressed that the quantitative analyses discussed below are specific to the methods used in this paper. The extent to which these results apply to other methodologies was not investigated here and would deserve further study before any conclusion can be drawn for MEG RSNs extracted, e.g., from CTF systems.

Interestingly, a highly significant sigmoidal relation was observed between spatial similarity indices and mean connectivity levels. This finding is of particular interest since these two aspects of rsFC could a priori fluctuate independently as spatial correlation between two maps is unaffected by linear transformation. This relation can be easily under-

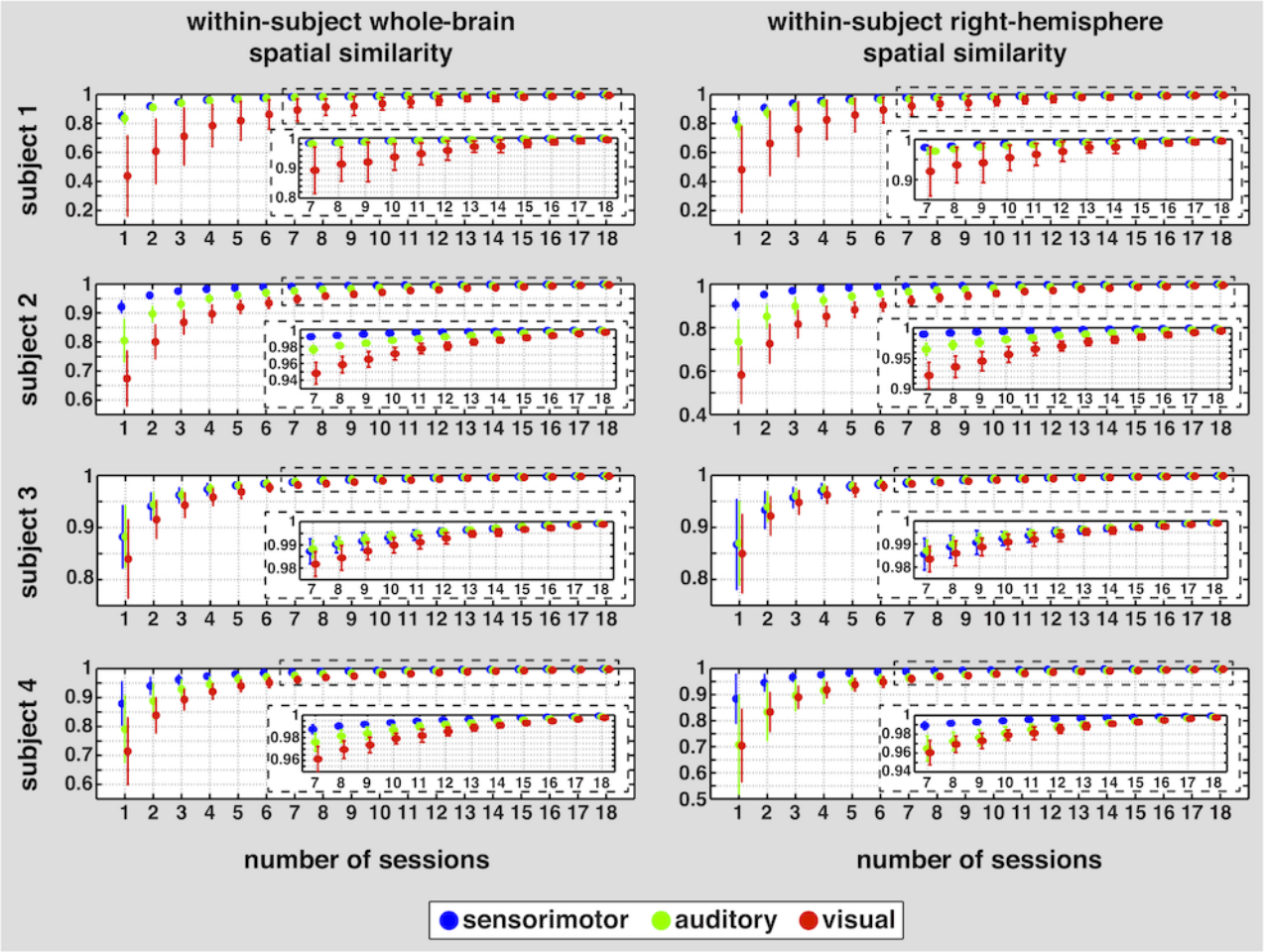

Fig. 8 Mean ± standard deviation of whole-brain (*left*) and right-hemisphere (*right*) within-subject spatial similarities of multiple sessions maps as a function of the number N of sessions. The means and standard deviations were estimated using 20 sessions ($N = 1$) or 150 randomly chosen subsets of sessions ($N \geq 2$). Insets zoom on values of $N \geq 7$

stood. Indeed, when within-network connectivity is too low, rsFC is dominated by noise, hence inducing a low spatial similarity with the canonical RSN. Spatial similarity increases with within-network connectivity, as the ratio of genuine connectivity to noise connectivity becomes larger, until it saturates to a maximal value. Spatial similarity becomes independent of within-network connectivity once in this saturation domain, indicating that connectivity noise is too low to contribute to RSN topography. This result makes the variations in RSN topography and in their connectivity level inter-related (although not equivalent in view of the saturation domain). Of notice, at the single-subject level where resting state data were sampled from multiple sessions, these relations were less clear; i.e., they were still observed within some individuals but with smaller p-values than across subjects, not in others, with no clear pattern emerging. This suggests that the intra-subject component of RSN variability makes their topographical pattern and their connectivity level fluctuate in a less correlated manner than the inter-subject component.

To investigate further the possible causes of individual RSN variability, the existence of a relation with various parameters has been explored. RSNs were found likely independent of most parameters considered in this study, which therefore allowed us to exclude several possible sources of variability such as raw MEG data quality. This latter finding suggests that artifact rejection (signal space separation, ICA) and head movement correction procedures efficiently subtract artifactual signals from raw data and do not impair RSN extraction. The absence of a relation with some of those parameters also has a practical impact on the experimental design of MEG RSN studies. An obvious potential source of RSN variability in the resting state data used in this study could result from gathering data from 4 different studies that were performed by various experimenters and used different experimental designs (e.g., cross fixation on a screen versus merely gazing at a point; resting state ses-

sion performed before, after, or randomized with, other task-specific sessions). However, the effect of the experimental condition on individual RSN spatial similarities and connectivity level was not found significant here. The present study was limited to the three RSNs associated with primary cortices (SM1, A1 and V1), even though additional higher-level associative MEG RSNs have also been identified at the group level (Brookes et al. 2011; Brookes et al. 2012b; de Pasquale et al. 2010; Hipp et al. 2012). Those networks, such as the DMN, are known to be affected by the experimental condition and previous cognitive tasks (Yan et al. 2009). Extending this study to higher-level associative RSNs would therefore require a dedicated study with better control on the experimental condition.

Power correlates of individual RSN topography and their connectivity level were also considered. This aspect is interesting to explore in order to further understand the neurophysiological basis of RSNs, and in particular their dependence on brain states, since the latter are known to be closely related to power levels in specific frequency bands. In principle, power correlates of rsFC allow investigation of this question, since the scale invariance of correlation implies that, in the absence of such underlying dependencies, rsFC as calculated from envelope correlation between sources oscillations is independent of their absolute power. In practice, however, higher source power generates a higher signal to noise ratio, which could thus affect rsFC estimates (Schoffelen and Gross 2009). No clear rule emerged from the Spearman correlation analysis between spatial similarities or within-network connectivity level and RSNs band-limited power levels, either at the inter- or intra-subject level. Yet, the absence of correlation with band-limited power levels does not preclude a relation with their ratios, which are known to be influenced by eyes closure or the subject's state of vigilance. The results showed no clear relation between spatial similarities or within-network connectivity levels and individual RSN power levels for the 2 RSNs computed from β band rhythms (SM1 and A1), suggesting that eye-closure or vigilance state (which were not monitored properly in this study) are not an important confound when studying these RSNs. On the other hand, a clearly significant relation was found for the V1 RSN, which was derived from α band neural oscillations, and indicated that spatial similarity for the V1 RSN improves as the α/θ and α/β power ratios increase. This might suggest that opening the eyes or a decrease in vigilance has a negative impact on the V1 RSN, but this clearly needs further investigations before drawing firm conclusions. Of notice, this relationship was not significant at the intra-subject level.

Another point of practical interest that needs to be considered is the impact of RSN variability on group level RSN studies. Indeed, variability might induce a loss of sensitivity when comparing RSNs across groups or conditions, since the effects sought may be smaller than the natural variability. It may therefore be mandatory in some studies to include a sufficient number of subjects in order to average out random fluctuations and isolate the effect of interest. Although the required number of subjects will in general depend on the investigation, rather conservative estimates were derived in this paper in a heuristic manner for each RSN. The consistency of group level MEG RSNs associated with primary cortices with $N \geq 12$ subjects is in line with the consistency of RSNs derived from ICA across two groups of $N = 10$ subjects described in the supplementary material of Brookes et al. (2011). Of course, the number of subjects could in principle be reduced if certain parameters at the origin of RSN variability could be controlled and optimized. For example, if the genuinely inter-subject component could be isolated within each subject (by averaging over multiple sessions), the required number of subjects could decrease.

In the above considerations, RSNs extraction was performed on the basis of template seeds common to all subjects. This potentially induces an over-estimation of RSNs variability associated with, e.g., inter-subject structural or functional anatomical differences in the location of primary cortices across individuals and possible suboptimal co-registration between MEG and MRI coordinate systems. In particular, the analysis based on template seeds yielded quite conservative upper bounds for the number of subjects (or sessions when considering intra-subject variability, see below) needed to average out RSNs variability. To obtain a more complete picture, analyses were repeated using a seed optimization method based on spatial similarity maximization. This procedure was defined in order to bias single-subject RSNs topography towards the canonical RSNs topography, hence yielding an under-estimation of RSNs variability. In particular, the ensuing evaluation of the number of subjects (or sessions) needed to average out RSNs variability was smaller and can be taken as a lower bound estimate. Comparison of these two approaches (template versus optimization) therefore gives a more complete picture of true RSNs variability, which should lie somewhat in between. A direct approach to avoid seed mislocation and get closer evaluation of true RSNs variability, would be to determine the right seed locations for each subject using functional localizers, as in Brookes et al. (2012b) for the SM1 RSN. This method was not used here, since this may be difficult to do when coming to clinical applications with patients having difficulties in performing tasks and it would decrease the obvious practical interest of resting state investigations; i.e., they do not require any explicit task.

4.2 Intra-subject and inter-subject variability

To investigate and compare the intra- and inter-subject components of RSN variability, data were acquired and analyzed

in 4 subjects that performed multiple resting state sessions in one day. The contribution of intra-subject variability was analyzed in this paper in a subject-specific manner using spatial similarity indices. In particular, within-subject spatial similarities were used to compare single-session connectivity maps and their within-subject average over the day. Their distribution across sessions was considered to quantify the intra-subject (or inter-session) variations of single-session RSN topographies. The validity of this subject-specific analysis based on within-subject spatial similarities requires that the within-subject average RSNs correctly represent the underlying individual RSN. To approach this ideal situation, the number of resting state sessions performed by each subject was chosen greater than the largest number of subjects necessary to obtain reproducible group level RSNs. Since $N = 12$ subjects were found to be sufficient to average out all RSNs fluctuations, 20 sessions are presumably sufficient to average out their intra-subject component only. On the basis of this analysis, the SM1 and A1 RSNs were found to be very robust and the V1 RSN least robust against intra-subject variations. On the other hand, the intra-subject variations varied with the subject, which suggests the existence of an interaction between inter- and intra-subject variability.

As discussed above, intra-subject variability only induces a mild co-variation between single-session RSN topography and their connectivity level, and none with the time of acquisition or their power levels and ratios (except in some subjects but with no clear rule). More generally, the question of the effect of time on individual RSNs can be considered. Variations of RSNs across sessions, and thus their temporal fluctuations on a very slow time scale (about one sample every 20 min), may a priori contain both random and temporally structured components. Examples of the latter include an effect of the circadian cycle on RSNs, or a specific trend in weariness of the subject as the day goes by. However, no such temporal structure could be found. In practice, this suggests that when studying the three RSNs considered in this study, resting state data can be acquired anytime during the day without significantly influencing RSNs. In theory, part of intra-subject fluctuations may originate from slow non-stationarities in rsFC, which would therefore constitute an irreducible source of variability. Indeed, even though this paper focused on a stationary rsFC estimate in which relatively rapid ($\sim$ 10 s) dynamic variations (de Pasquale et al. 2010; de Pasquale et al. 2012) were smoothed out, the finite length of the data did not preclude non-stationarities over longer time scales (a few minutes). The origins and properties of such hypothetic very slow dynamic fluctuations (< 0.01 Hz) in source envelope rsFC remain unexplored and would need to be investigated conjointly with the other known properties of RSNs; e.g., through the explicit inclusion of long-lasting neuromodulatory effects in the large-scale neural models reviewed in Deco et al. (2011). In this context, the present discussion suggests that very slow non-stationary rsFC variations within the SM1, A1 and V1 RSNs, if they exist, do not exhibit temporal autocorrelations and can be described as white processes at those time scales. However, this would need to be investigated more carefully before any firm conclusions may be drawn on this topic, since other uncontrolled sources of variability might also contribute to intra-subject variability. Studying this latter question is an interesting technical issue that was not addressed in this work.

Averaging out inter-session fluctuations appears useful when comparing RSNs across subjects or conditions at the individual level. Two simple ways to achieve this goal are either to average over multiple sessions or to increase the resting state acquisition length. The first approach was considered in this work by using fixed-length (5 min) sessions. Although the minimal number of sessions needed to average out intra-subject fluctuations depends both on the RSN and the subject (since inter-subject RSN variability influences intra-subject RSNs variability), conservative estimates were derived in this paper. These estimates ($2 \leq N \leq 11$) can be compared with analogous studies on BOLD rsFC. For example, Anderson et al. (2011) found that 5 sessions are required to reliably extract BOLD RSNs in a single subject using ICA. The second method to dampen intra-subject variations was recently studied in fMRI in Birn et al. (2013), which suggested that increasing the scan length yields more reliable estimates of BOLD rsFC than using multiple sessions. Furthermore, Damoiseaux et al. (2006) derived BOLD RSNs from 40 min-long resting state sessions in 10 subjects acquired twice, and showed them to be highly consistent across subjects and time. In light of these comments, it would be interesting to explicitly study the effect of session length in the context of MEG RSNs, which was not done in this study.

The averaging procedure over sessions within the 4 considered subjects also allowed isolation of the inter-subject component of RSNs variability across them. Although the small number of subjects involved in this paper limits analyses, the existence of a significant inter-subject variability on top of intra-subject fluctuations was found. However, a detailed comparison of inter- and intra-subject would require extending the analysis to more than 4 subjects.

5 Conclusions

This study systematically investigates the robustness and variability of the SM1, A1 and V1 MEG RSNs derived from seed-based envelope correlation. Two estimations of RSNs variability are given, one based on template MNI seeds, which potentially over-estimates variability due to seed mislocation, and the other based on optimized seeds, which bias RSNs extraction towards minimal variability. True RSNs variability should lie in between.

The main finding is that inter- and intra-subject variability is substantial and non-trivial, especially for the A1 and V1 RSNs, but can however be dampened by averaging over a reasonable ($N \sim 10$) number of subjects or sessions. Interestingly, MEG RSNs seem unaffected by many features of resting state acquisition as neither the raw MEG data quality, the experimental condition, the moment of acquisition, the power levels nor the power band ratios had significant effects on MEG RSNs topography, except for power band ratios on the V1 RSN.

Therefore, MEG appears to be a valid technique to study and use RSNs at least for networks associated with primary cortices and upon sufficient averaging and critically complements the more classical resting state fMRI studies by allowing exploration of the spatiotemporal brain dynamics underlying the emergence and potential functions of RSNs. This study suggests practical implications for the potential use of MEG RSNs in single-subject studies based on Vectorview Elekta Neuromag systems and wMNE source modeling, particularly in clinics where diagnostic, prognostic or therapeutic applications should be restricted to a single and relatively short resting state MEG session.

Acknowledgements Mathieu Bourguignon (research fellow) benefits from a research grant from the Fonds pour la Formation la Recherche dans l'Industrie et dans l'Agriculture (FRIA, FRS-FNRS, Belgium). Catherine Clumeck (research fellow), Alison Mary (research fellow) and Xavier De Tiège (post-doctorate clinical caster specialist) benefit from a research grant from the Fonds de la Recherche Scientifique (FRS-FNRS, Belgium). Matthew J. Brookes is funded by a Leverhulme Trust Early Career Fellowship. This work was supported by research grants from the Fonds de la Recherche Scientifique (research conventions: 3.4811.08, 3.4547.10, 3.4554.12; FRS-FNRS, Belgium).

References

1. Anderson JS, Ferguson MA, Lopez-Larson M, Yurgelun-Todd D (2011) Reproducibility of single-subject functional connectivity measurements. AJNR Am J Neuroradiol 32 (3):548-555. doi:10.3174/ajnr.A2330
2. Birn RM, Molloy EK, Patriat R, Parker T, Meier TB, Kirk GR, Nair VA, Meyerand ME, Prabhakaran V (2013) The effect of scan length on the reliability of resting-state fMRI connectivity estimates. Neuroimage 83:550-558. doi:10.1016/j.neuroimage.2013.05.099
3. Biswal B, Yetkin FZ, Haughton VM, Hyde JS (1995) Functional connectivity in the motor cortex of resting human brain using echo-planar MRI. Magn Reson Med 34 (4):537-541
4. Brockwell PJ, Davis RA (1987) Model building and forecasting with ARIMA processes. In: Brockwell PJ, Davis RA (eds) Times series: theory and methods. Springer-Verlag, New York, pp 265 - 319
5. Brookes MJ, Liddle EB, Hale JR, Woolrich MW, Luckhoo H, Liddle PF, Morris PG (2012a) Task induced modulation of neural oscillations in electrophysiological brain networks. Neuroimage 63 (4):1918-1930. doi:10.1016/j.neuroimage.2012.08.012
6. Brookes MJ, Woolrich M, Luckhoo H, Price D, Hale JR, Stephenson MC, Barnes GR, Smith SM, Morris PG (2011) Investigating the electrophysiological basis of resting state networks using magnetoencephalography. Proc Natl Acad Sci U S A 108 (40):16783-16788. doi:10.1073/pnas.1112685108
7. Brookes MJ, Woolrich MW, Barnes GR (2012b) Measuring functional connectivity in MEG: a multivariate approach insensitive to linear source leakage. Neuroimage 63 (2):910-920. doi:10.1016/j.neuroimage.2012.03.048
8. Carrette E, Op de beeck M, Bourguignon M, Boon P, Vonck K, Legros B, Goldman S, Van Bogaert P, De Tiège X (2011) Recording temporal lobe epileptic activity with MEG in a light-weight magnetic shield. Seizure 20 (5):414-418. doi:10.1016/j.seizure.2011.01.015
9. D'Esposito M, Deouell LY, Gazzaley A (2003) Alterations in the BOLD fMRI signal with ageing and disease: a challenge for neuroimaging. Nat Rev Neurosci 4 (11):863-872. doi:10.1038/nrn1246 Dale AM, Sereno MI (1993) Improved localization of cortical activity by combining EEG and MEG with MRI cortical surface reconstruction: A linear approach. J Cogn Neurosci 5:162-176
10. Damoiseaux JS, Rombouts SA, Barkhof F, Scheltens P, Stam CJ, Smith SM, Beckmann CF (2006) Consistent resting-state networks across healthy subjects. Proc Natl Acad Sci U S A 103 (37):13848-13853. doi:10.1073/pnas.0601417103
11. de Pasquale F, Della Penna S, Snyder AZ, Lewis C, Mantini D, Marzetti L, Belardinelli P, Ciancetta L, Pizzella V, Romani GL, Corbetta M (2010) Temporal dynamics of spontaneous MEG activity in brain networks. Proc Natl Acad Sci U S A 107 (13):6040-6045. doi:10.1073/pnas.0913863107
12. de Pasquale F, Della Penna S, Snyder AZ, Marzetti L, Pizzella V, Romani GL, Corbetta M (2012) A cortical core for dynamic integration of functional networks in the resting human brain. Neuron 74 (4):753-764. doi:10.1016/j.neuron.2012.03.031
13. De Tiège X, Op de beeck M, Funke M, Legros B, Parkkonen L, Goldman S, Van Bogaert P (2008) Recording epileptic activity with MEG in a light-weight magnetic shield. Epilepsy Res 82 (2-3):227-231. doi:10.1016/j.eplepsyres.2008.08.011
14. Deco G, Corbetta M (2011) The dynamical balance of the brain at rest. Neuroscientist 17 (1):107-123. doi:10.1177/1073858409354384
15. Deco G, Jirsa VK, McIntosh AR (2011) Emerging concepts for the dynamical organization of resting-state activity in the brain. Nat Rev Neurosci 12 (1):43-56. doi:10.1038/nrn2961
16. Del Gratta C, Pizzella V, Tecchio F, Romani GL (2001) Magnetoencephalography–a noninvasive brain imaging method with 1 ms time resolution. Rep Prog Phys 64:1759-1814
17. Fox MD, Greicius M (2010) Clinical applications of resting state functional connectivity. Front Syst Neurosci 4:19. doi:10.3389/fnsys.2010.00019
18. Fox MD, Raichle ME (2007) Spontaneous fluctuations in brain activity observed with functional magnetic resonance imaging. Nat Rev Neurosci 8 (9):700-711. doi:nrn2201 [pii]
19. Hall EL, Robson SE, Morris PG, Brookes MJ (2013a) The relationship between MEG and fMRI. Neuroimage:In Press
20. Hall EL, Woolrich MW, Thomaz CE, Morris PG, Brookes MJ (2013b) Using variance information in magnetoencephalography measures of functional connectivity. Neuroimage 67:203-212. doi:10.1016/j.neuroimage.2012.11.011
21. Hämäläinen M, Hari R, Ilmoniemi RJ, Knuutila J, Lounasmaa OV (1993) Magnetoencephalographytheory, instrumentation, and applications to noninvasive studies of the working human brain. Rev Mod Phys 65 (2):413-497
22. Hämäläinen M, Lin F, Mosher JC (2010) Anatomically and functionally constrained minimum-norm estimates. In: Hansen PC, Kringelbach ML, Salmelin R (eds) MEG – An introduction to methods. Oxford University Press, pp 186 - 215
23. Hawellek DJ, Schepers IM, Roeder B, Engel AK, Siegel M, Hipp JF (2013) Altered intrinsic neuronal interactions in the visual cortex of the blind. J Neurosci 33 (43):17072-17080. doi:10.1523/JNEUROSCI.1625-13.2013
24. Hipp JF, Hawellek DJ, Corbetta M, Siegel M, Engel AK (2012) Large-scale cortical correlation structure of spontaneous oscillatory activity. Nat Neurosci 15 (6):884-890. doi:10.1038/nn.3101

25. Hutchison RM, Womelsdorf T, Allen EA, Bandettini PA, Calhoun VD, Corbetta M, Della Penna S, Duyn JH, Glover GH, Gonzalez-Castillo J, Handwerker DA, Keilholz S, Kiviniemi V, Leopold DA, de Pasquale F, Sporns O, Walter M, Chang C (2013) Dynamic functional connectivity: promise, issues, and interpretations. Neuroimage 80:360-378. doi:10.1016/j.neuroimage.2013.05.079
26. Lindauer U, Dirnagl U, Fuchtemeier M, Bottiger C, Offenhauser N, Leithner C, Royl G (2010) Pathophysiological interference with neurovascular coupling - when imaging based on hemoglobin might go blind. Front Neuroenergetics 2. doi:10.3389/fnene.2010.00025
27. Liu TT (2013) Neurovascular factors in resting-state functional MRI. Neuroimage 80:339-348. doi:10.1016/j.neuroimage.2013.04.071
28. Luckhoo H, Brookes MJ, Heise V, Mackay CE, Ebmeier K, Morris PG, Woolrich MW Extracting resting state networks from Elekta Neuromag MEG data using independent component analysis. In: 18th Annual Meeting of the Organization for Human Brain Mapping, Beijing, 2012a.
29. Luckhoo H, Hale JR, Stokes MG, Nobre AC, Morris PG, Brookes MJ, Woolrich MW (2012b) Inferring task-related networks using independent component analysis in magnetoencephalography. Neuroimage 62 (1):530-541. doi:10.1016/j.neuroimage.2012.04.046
30. Marzetti L, Della Penna S, Snyder AZ, Pizzella V, Nolte G, de Pasquale F, Romani GL, Corbetta M (2013) Frequency specific interactions of MEG resting state activity within and across brain networks as revealed by the multivariate interaction measure. Neuroimage 79:172-183. doi:10.1016/j.neuroimage.2013.04.062
31. O'Neill G, Hall E, Corner SP, Morris PG, Brookes MJ A comparison of beamformer and minimum norm solutions for network mapping in MEG. In: 19th Annual Meeting of the Organization for Human Brain Mapping, Seattle, WA, 2013.
32. Oldfield RC (1971) The assessment and analysis of handedness: the Edinburgh inventory. Neuropsychologia 9 (1):97-113
33. Raichle ME (2010) Two views of brain function. Trends Cogn Sci 14 (4):180-190. doi:10.1016/j.tics.2010.01.008
34. Schoffelen JM, Gross J (2009) Source connectivity analysis with MEG and EEG. Hum Brain Mapp 30 (6):1857-1865. doi:10.1002/hbm.20745
35. Scholvinck ML, Leopold DA, Brookes MJ, Khader PH (2013) The contribution of electrophysiology to functional connectivity mapping. Neuroimage 80:297-306. doi:10.1016/j.neuroimage.2013.04.010
36. Stam CJ (2005) Nonlinear dynamical analysis of EEG and MEG: review of an emerging field. Clin Neurophysiol 116 (10):2266-2301. doi:10.1016/j.clinph.2005.06.011
37. Taulu S, Simola J, Kajola M (2005) Applications of the signal space separation method. IEEE Trans Sign Proc 53:3359-3372
38. Vigario R, Sarela J, Jousmaki V, Hamalainen M, Oja E (2000) Independent component approach to the analysis of EEG and MEG recordings. IEEE Trans Biomed Eng 47 (5):589-593. doi:10.1109/10.841330
39. Yan C, Liu D, He Y, Zou Q, Zhu C, Zuo X, Long X, Zang Y (2009) Spontaneous brain activity in the default mode network is sensitive to different resting-state conditions with limited cognitive load. PLoS One 4 (5):e5743. doi:10.1371/journal.pone.0005743

Supplementary materials

S1 Regions of interest used for seed optimization

See Figure S1.

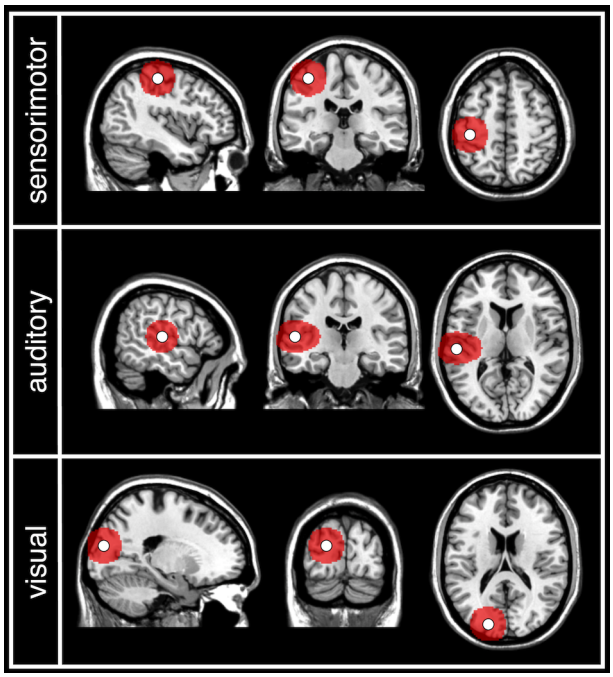

Fig. S1 To apply the seed optimization method, regions of interest were defined in the MNI brain as spheres or ellipsoids (*red*) centered on the template seeds (*white*). These regions contained 123 (SM1), 110 (A1) and 119 (V1) different sources. The corresponding sources, mapped onto each subject's brain, were then used for single-subject connectivity analysis

S2 Examples of individual and group level connectivity maps

See Figure S2.

S3 Relation between RSN mean connectivity and power levels

After Bonferroni correction for $n = 6$ comparisons (6 power levels and ratios), significant power correlates of within-network connectivity levels were found in the SM1 RSN with the β/θ power ratio ($p < 4 \times 10^{-3}$, uncorrected), and in the V1 RSN with the α/θ and α/β power ratios ($p < 10^{-5}$, uncorrected). Without correction, a tendency for significance was also observed with the α/β power ratio in the SM1 RSN, and with the α/θ and β/θ power ratios in the A1 RSN, and with the α power in the V1 RSN ($p < 0.04$, uncorrected). All other correlations had uncorrected p-values above 0.11.

S4 Redundancy of the resampling analysis plot (Figure 4)

The description presented in Figure 4 is redundant. The values for the mean and standard deviation of spatial similarities for $1 \leq N \leq 30$ are actually inter-related, and only de-

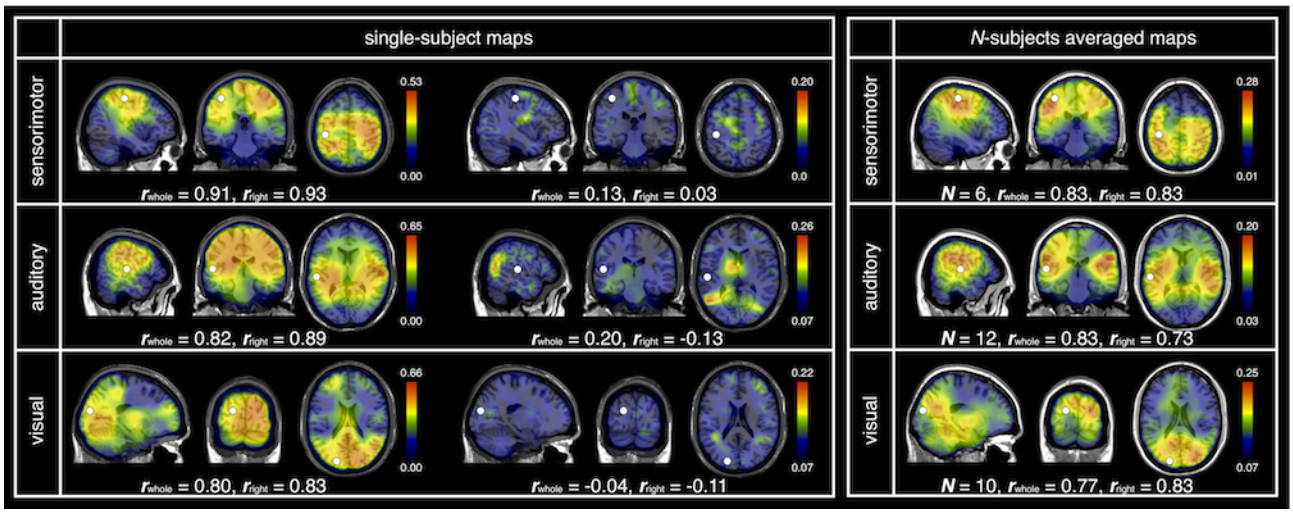

Fig. S2 Examples of single-subject (single session) and size N group level connectivity maps, superimposed on the MNI brain. The template seeds are indicated as white dots. The lower and upper thresholds are respectively fixed at the minimum and maximum of connectivity. The envelope correlation values indicated are uncorrected for the orthogonalization bias (Hipp et al. 2012). The values of whole-brain (r_{whole}) and right-hemisphere (r_{right}) spatial similarities with the associated canonical RSN are also indicated below the corresponding maps. **Left:** The two single-subject maps with the highest (*left*) and lowest (*right*) average spatial similarity $r_{\text{mean}} = (r_{\text{whole}} + r_{\text{right}})/2$ across the 58 subjects. **Right:** The size N group level map with lowest r_{mean} among the 1000 group maps obtained using the resampling analysis for a given population size N (chosen according to the results of Section 3.1.5)

pend on the standard deviation of individual (single session, $N = 1$) maps spatial similarities, as illustrated in Figure S4 for whole-brain spatial similarity. Results for right-hemisphere spatial similarities are analogous.

Despite this redundancy, this description involves a rearrangement of the information contained in spatial similarities that is useful to quantify how group averaging dampens inter-subject variability as a function of the number of subjects.

S5 Relation between RSN topography and raw MEG data quality

To assess to which extent spatial similarity indices are related to raw MEG data quality, the ratio of mean gradiometers variance of raw data (no artifact correction, no signal space separation, no movement compensation and no ICA; but data filtered between 0.5 Hz and 45 Hz) to mean gradiometers variance of artifact-cleaned data was computed. To assess the effect of subject's head movement, the variance of the 6 quaternions parameters (3 rotation, 3 translation) describing the subject's frame (Besl and McKay 1992) was computed using the head movement estimation based on signal space separation (Taulu et al. 2005; Uutela et al. 2001). The existence of a relation between spatial similarities and these indices was tested using Spearman rank correlation. Even without correction for multiple comparisons, this analysis did not reveal a significant relation between spatial similarities and fraction of data variance removed by artifact correction or subject's head movement parameters ($p > 0.08$, uncorrected).

S6 Dependence of RSN on experimental condition

The resting state MEG data used in this paper came from 4 different studies investigating either the cortico-kinematic (9 subjects) (Bourguignon et al. 2011) or cortico-vocal (10 subjects) (Bourguignon et al. 2013) coherence phenomena, the effect of procedural memory consolidation on central μ rhythm (15 subjects) (Mary et al. 2013), or central μ rhythm modulations by various sensorimotor stimulations (24 subjects, data under analysis). Resting state sessions were acquired in a randomized order relative to task- or stimulus-driven sessions in three studies, and were always acquired first in one study (procedural memory consolidation). We will refer to this as the experimental condition of the resting state session.

Considering the potential influence of previous behavioral tasks on RSNs (for a review, see Deco and Corbetta (2011)), the effect of the experimental condition on single session RSNs (58 subjects gathered from 4 studies) was investigated by applying a non-parametric Kruskal-Wallis one-way ANOVA test on single session spatial similarities and within-network connectivity levels, after partitioning them into the 4 subpopulations (of respective sizes 9, 10, 15, 24) corresponding to each MEG study in which resting state data were recorded.

These ANOVA tests did not reveal a significant effect of the experimental condition either for whole-brain or right-

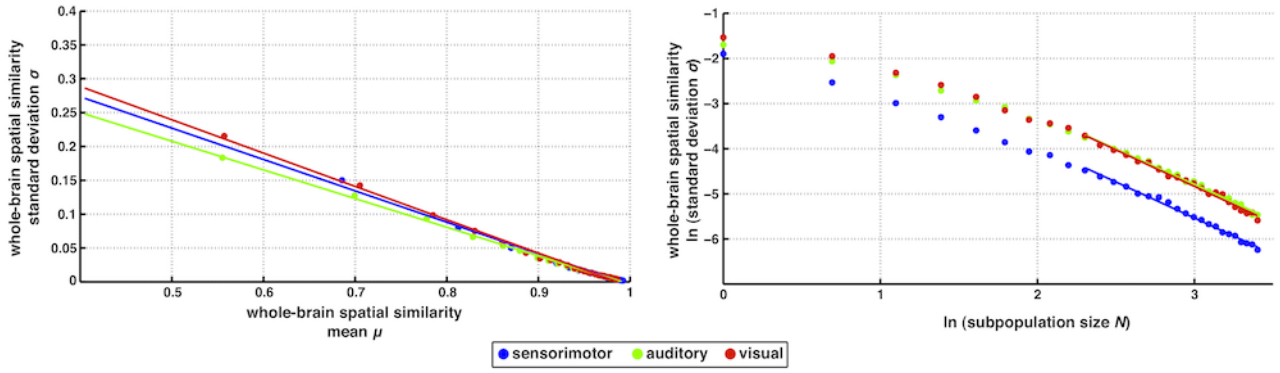

Fig. S4 Left: The plot of the 30 standard deviations σ of whole-brain spatial similarity of size N subpopulation maps as a function of their mean μ shows that they are linearly related. For each RSN, a model $\sigma(\mu) = a(1-\mu)$ was fitted using linear regression (SM1: $a = 0.46$; A1: $a = 0.42$; V1: $a = 0.49$). **Right:** A log-log plot of σ versus N shows that σ converges to zero as N increases. For N large enough, this convergence takes place according to a power law $\sigma(N) = N^{-k}$ whose exponent was estimated for each RSN from a log-log linear regression restricted to $N \geq 10$ (SM1: $k = 1.60$; A1: $k = 1.58$; V1: $k = 1.62$). This shows that the variables $\sigma(N)$ (and thus $\mu(N)$) only depend on the value of $\sigma(N = 1)$, quite independently of the RSN in view of the similarity in the estimates of a and k

hemisphere spatial similarities ($p > 0.13$ for all RSNs), or for within-network connectivity levels ($p > 0.28$ for the SM1 and A1 RSNs; $p = 0.06$ for the V1 RSN, indicating a possible trend in this case).

S7 Resampling analysis plot for seed optimized maps

See Figure S7.

S8 Distribution of spatial similarities with canonical RSNs across sessions

See Figure S8.

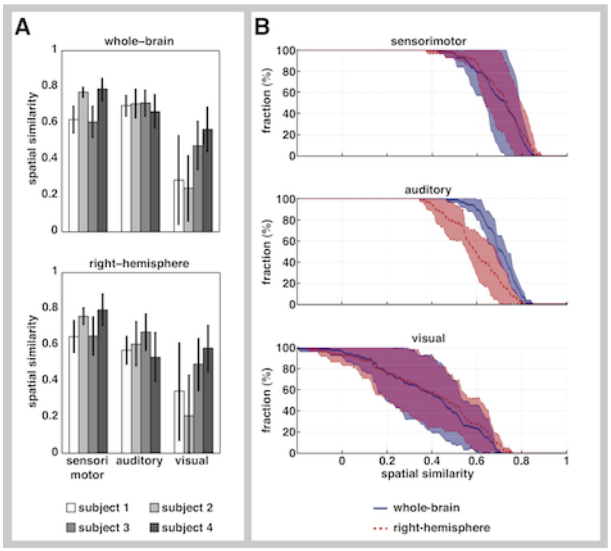

Fig. S8 Mean ± standard deviation over sessions (within each subject) of whole-brain and right-hemisphere spatial similarities of single session connectivity maps with canonical maps (**A**), and mean ± standard deviation over the 4 subjects of the fraction of sessions with within-subject spatial similarities above given values (**B**)

S9 Relations between multiple sessions RSN topography, mean connectivity levels and mean power levels

The mean connectivity level of multiple sessions connectivity maps (derived from $N = 1$ session) and the associated band-limited power levels and ratios were computed as in Section 2.5.3 for each subject, RSN and session. The existence of a relation between these parameters and within-subject spatial similarities was tested using Spearman rank correlation.

At the level of intra-subject fluctuations, the clear dependence between the spatial similarities and within-network connectivity level observed in Section 3.1.3 was not preserved in all subjects. Indeed, such relations could be deduced in all subjects except 3 for the SM1 RSN and 2 for the V1 RSN, for which whole-brain and right-hemisphere spatial similarities were not correlated with within-network connectivity level ($p > 0.06$, uncorrected).

No clear and systematic relation could be observed between spatial similarities and mean power levels or their ratios, or between within-network connectivity and mean power levels or their ratios.

S10 Resampling analysis plot for seed-optimized within-subject spatial similarities

See Figure S10.

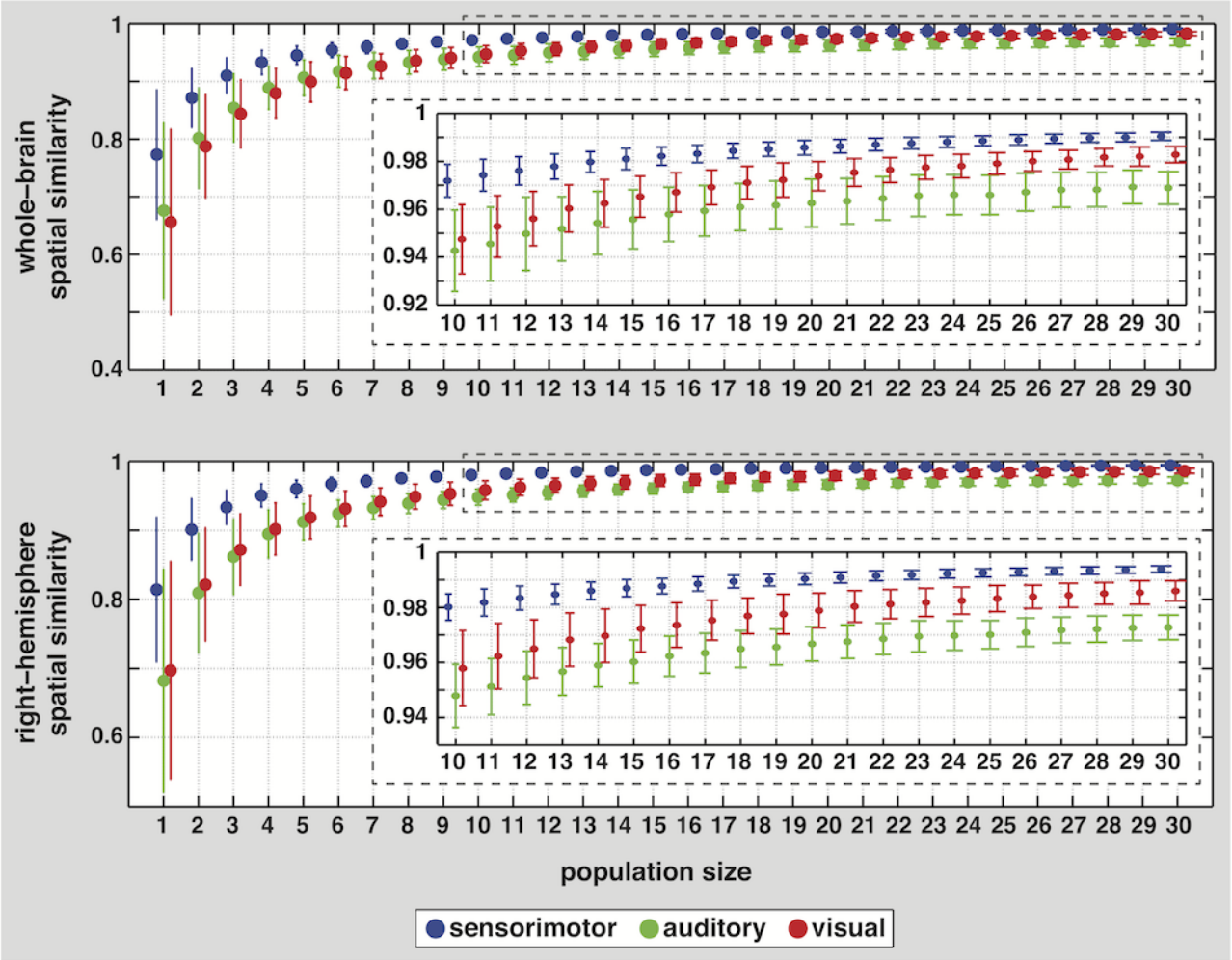

Fig. S7 Mean ± standard deviation of whole-brain (*top*) and right-hemisphere (*bottom*) spatial similarities between size N group connectivity maps ($1 \leq N \leq 30$) derived from optimized seeds and the associated canonical map, as a function of the population size N. The means and standard deviations were estimated using single sessions obtained in 58 subjects ($N = 1$) or 1000 randomly chosen subpopulations ($N \geq 2$). The insets zoom on values of $N \geq 10$. It follows from the distributions depicted in **B** that, amongst the 20 sessions, 53% 46% of the SM1 maps, 21% 22% of the A1 maps and none of the V1 maps presented both whole-brain and right-hemisphere spatial similarities with the canonical RSN above 0.7

References for supplementary materials

1. Besl PJ, McKay ND (1992) A method for registration of 3-D shapes. IEEE Trans Patt Anal Machine Intell 14:239-255
2. Bourguignon M, De Tiège X, Op de Beeck M, Ligot N, Paquier P, Van Bogaert P, Goldman S, Hari R, Jousmäki V (2013) The pace of prosodic phrasing couples the listener's cortex to the reader's voice. Hum Brain Mapp 34 (2):314-326
3. Bourguignon M, De Tiège X, Op de Beeck M, Pirotte B, Van Bogaert P, Goldman S, Hari R, Jousmäki V (2011) Functional motor-cortex mapping using corticokinematic coherence. Neuroimage 55 (4):1475-1479
4. Deco G, Corbetta M (2011) The dynamical balance of the brain at rest. Neuroscientist 17 (1):107-123.
5. Mary A, Bourguignon M, Op de Beeck M, Leproult R, De Tiège X, Peigneux P (2013) Ageing experience-induced sensorimotor plasticity. A magnetoencephalographic study. Submitted
6. Taulu S, Simola J, Kajola M (2005) Applications of the signal space separation method. IEEE Trans Sign Proc 53:3359-3372
7. Uutela K, Taulu S, Hämäläinen M (2001) Detecting and correcting for head movements in neuromagnetic measurements. Neuroimage 14 (6):1424-1431

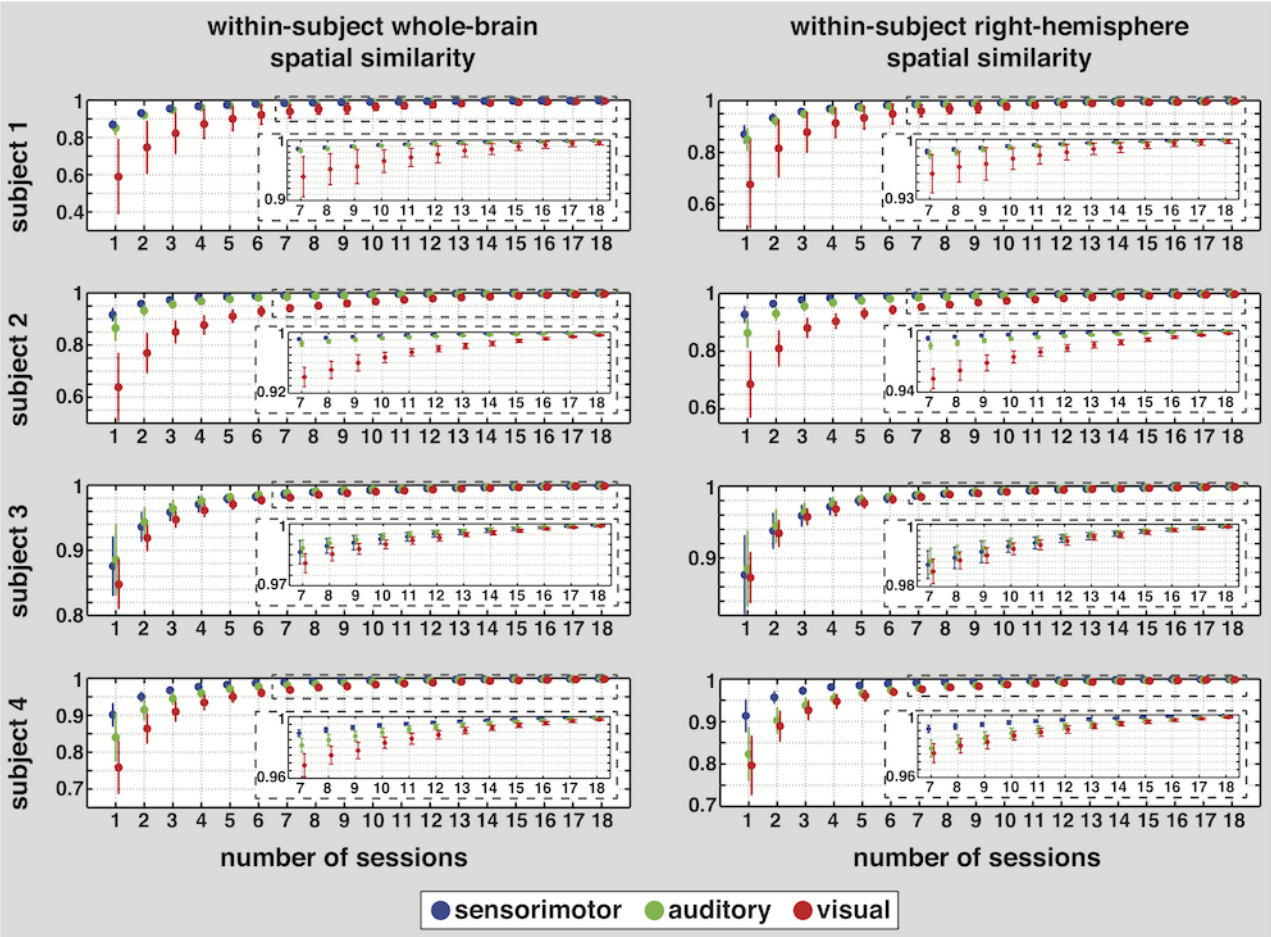

Fig. S10 Mean ± standard deviation of whole-brain (*left*) and right-hemisphere (*right*) within-subject spatial similarities of multiple sessions maps with seed optimization, as a function of the number N of sessions. The means and standard deviations were estimated using 20 sessions ($N = 1$) or 150 randomly chosen subsets of sessions ($N \geq 2$). Insets zoom on values of $N \geq 7$